# A Novel Microfluidic Multichannel Electrochemical Cell for Multiplexed Monitoring of Water Pollutants

Tong Liu (liu@ufe.cz), Ivo Tichý(tichy@ufe.cz), Jiří Homola*(homola@ufe.cz), Amir M. Ashrafi*(ashrafi@ufe.cz)

*Institute of Photonics and Electronics, Czech Academy of Sciences, Chaberská 1014/57, 182 51, Prague, Czech Republic.*

## *2.3 Methods*

### *2.3.1 Electrochemical cleaning of the electrodes.*

The assembled MMEC underwent electrochemical cleaning to ensure a clean gold surface. For this purpose, a 0.5 M $H_2SO_4$ solution was introduced into the MMEC, and cyclic voltammetry (CV) was performed for 20 cycles under the following conditions: starting potential 0.0 V, end potential +1.4 V, and scan rate 50 mV $s^{-1}$. Subsequently, the MMEC was rinsed by injecting deionized (DI) water through the system.

### *2.3.2 Electrochemical characterization*

Electrochemical characterization of fabricated MMEC was carried out by recording cyclic voltammograms in a solution of 1 mM $[Ru(NH)_3]^{2+/3+}$ and 100 mM KCl at different scan rates. The parameters of the recorded CVs were as follows: starting potential 0.0 V, end potential −0.4 V, and step potential 2 mV.

The crosstalk between the MMEC channels was investigated to ensure that the measurement in one channel does not affect the electrochemical responses on other channels. The chronopotentiograms at constant DC current of 0.5 µA were recorded at channels 2–4 while 0.1 KCl was introduced to the MMEC. After 120 s when reaching to the equilibrium was ensured in chronopotentiograms, recording CV was initiated in channel 1. To study the effect of recording CV in channel 1, the potential of the recorded chronopotentiograms in channels 2-4, the was subjected to Fourier analysis. Comparison of the FFT of residuals between the experimental and fitted data in the recorded chronopotentiograms, and the FFT of the CVs run in channel 1 shows the potential effect of CV in channel 1 on the chronopotentiograms in channels 2-4.

Chronopotentiometric measurements were conducted in channels 2–4 under a constant DC current of 0.5 µA, following the introduction of 0.1 M KCl into the MMEC system. After 120 s, once the system had reached electrochemical equilibrium cyclic voltammetry (CV) was initiated in channel 1. To investigate the potential influence of CV recording in channel 1 on the chronopotentiometric responses in channels 2–4, the recorded potentials were analyzed

*Corresponding authors: ashrafi@ufe.cz, homola@ufe.cz

using Fourier transform methods. A comparative analysis of the fast Fourier transforms (FFTs) of the residuals between the experimental and fitted chronopotentiometric data, alongside the FFT of the CV from channel 1, shows the potential influence of CV process in channel on the measurements in channels 2–4.

For calculation of effective surface area, the CVs of the corresponding electrode configuration were carried out at different scan rate in 4 mM $[Fe(CN)_6]^{3-/4-}$ and 100 mM KCl. The effective surface area then was calculated by using the slope of $I_p$ vs. $\nu^{0.5}$ and using Randles-Sevcik equation:

$$I_p = 0.4463\, nFAC\left(\frac{nF\nu D}{RT}\right)^{\frac{1}{2}}$$

Where $I_p$ is the peak current, $F$ is the Faraday constant, $A$ is the effective surface area of the electrode, $C$ is the concentration of the $[Fe(CN)_6]^{3-/4-}$, $n$ is the number of exchanged electrons, $D$ is the diffusion coefficient of the redox probe, $\nu$ is the scan rate, $R$ is the gas constant, and T is the temperature.

The electrochemical impedance spectroscopy (EIS) of different electrode configurations were recorded in 4 mM $[Fe(CN)_6]^{3-/4-}$ and 100 mM KCl. The *ac* potential amplitude of 5 mV was superimposed on open circuit potential (OCP) and the frequency was scanned from 100 kHz to 1 Hz. The obtained are presented in Nyquist plot where −imaginary part of impedance ($-Im(Z)/\Omega$) is plotted against the real part of impedance ($Re(Z)/\Omega$).

*2.3.3 Preparation of gold electrode modified with gold nanostructures (Au/AuNS)*

Gold nanostructures (AuNS) were electrochemically deposited onto the gold (Au) electrode by applying a potential of −0.30 V for a specified duration, while a 0.6 mM $HAuCl_4$ in 100 mM $KNO_3$ solution was delivered into the cell.

*2.3.4 Determination of $H_2O_2$*

Determination of $H_2O_2$ was carried out by chronoamperometry at Au electrode that had been electrodeposited with AuNS for 10 min. In chronoamperometry the potential was set at −0.30 V, and the current was sampled every 0.5 s. The supporting electrolyte in $H_2O_2$ determination was 100 mM KCl. After injecting the supporting electrolyte and reaching a steady–state current, the desired concentration of $H_2O_2$ was introduced into the cell by immersing the tube in the prepared analyte solution. Once a stable current response was achieved, the tube was transferred to the supporting electrolyte solution until the baseline current stabilized. No cleaning step was used for the electrode surface, because the reduction of $H_2O_2$ at Au/AuNS did not leave any residue.

*2.3.5 Determination of catechol*

First the gold electrode was deposited with a layer of polyurea (PU) by cycling the potential between −1.20 V and +0.80 V at a scan rate of 50 $mVs^{-1}$ while a solution of 2 mM urea in PBS pH 7.4 was directed to the cell. Thus prepared Au/PU was later modified with electrodeposition of AuNS for 2 min to obtain Au/PU/AuNS. The electrochemical determination of catechol was carried out at the prepared Au/PU/AuNS using square wave voltammetry (SWV) in 100 mM acetate buffer pH 5.7. with the following parameters, the starting potential −0.30 V, end potential +0.50 V, pulse amplitude 20 mV, step potential 3 mV, frequency 25 Hz.

*2.3.6 Determination of lead ions at gold electrode modified with mercury film (Au/MF)*

For the electrochemical determination of lead ions ($Pb^{2+}$), a mercury film (MF) was first electrodeposited onto the gold (Au) electrode to achieve (Au/MF). This process involved the use of a 100 ppm $Hg^{2+}$ solution in 1 mM $HNO_3$. To mitigate hydrogen evolution, a stepwise potential regime was employed, with potentials applied as follows: −0.7 V for 60 s, −0.8 V for 60 s, −0.9 V for 60 s, −1.0 V for 60 s, −1.1 V for 60 s, −1.2 V for 60 s, and −1.3 V for 120 s. This gradual deposition approach facilitated the controlled formation of the MF on the Au electrode surface, effectively shifting the onset of hydrogen evolution to more negative cathodic potentials. The electrochemical determination of $Pb^{2+}$ was carried out at so prepared Au/MF in 100 mM acetate buffer pH 4.5 by SWV with following parameters, cleaning potential −0.4 V for 90 s, accumulation potential −1.3 V for 180 s, start potential −1.3 V, end potential −0.1 V, pulse amplitude 50 mV, frequency 80 Hz.

*2.3.7 Determination of mercury ions ($Hg^{2+}$) at gold electrode*

Differential pulse voltammetry (DPV) was employed for determination of mercury ions at Au electrode in 100 mM HCl. The applied parameters of DPV were as follows: cleaning potential +0.6 V for 60 s, accumulation potential +0.3 V for 180 s, starting potential +0.3 V, end potential +0.8 V, pulse amplitude 70 mV, pulse time 5 ms, step potential 2 mV, scan rate 50 $mVs^{-1}$.

*2.3.8 Repeatability, reproducibility, limit of detection (LOD), and limit of quantification (LOQ)*

The precision of the results was justified by calculating the repeatability and reproducibility. The repeatability was calculated by performing 3 repetitive measurements without altering the measurement set up and reporting the corresponding RSD%. The reproducibility was investigated by repetitive measurements at 4 different electrodes. Reproducibility was reported as the RSD% of the results. The limit of detection (LOD) and limit of quantification (LOQ) were calculated as 3 *s*/*m,* and 10 *s*/m*,* respectively, where *s* represents the standard deviation of

3 repetitive measurements of the lowest concentration in the dynamic range, and *m* is the slope of the calibration curve.

*2.3.9 Interference study.*

To investigate the interference effect of the potential interfering compounds, an electrochemical measurement was carried out with a given concentration of an analyte. Another measurement was run after the addition of each interfering compound to the solution. The interfering effect was evaluated by percentage of current change. The concentration for the heavy metal ions ($Hg^{2+}$, $Pb^{2+}$, $As^{3+}$, $Zn^{2+}$, $Cd^{2+}$) was 50 ppb, and other chemicals NaCl, $MgCl_2$, $CaCl_2$, ureal, catechol, ascorbic acid, glucose, $H_2O_2$ organic compounds (ascorbic acid, glucose) was 50 μM.

*2.3.10 Recovery percentage and real sample analysis*

The accuracy of the developed methods was evaluated through recovery studies, which involved spiking buffer and river water sample (Vltava Prague, Czech Republic) with known concentrations of the analyte, followed by analysis using the developed methods. To eliminate the matrix effect the standard addition method was employed for concentration determination of analytes where the initial measurement was followed by two successive measurements after addition of known concentrations of the analyte to the sample a standard addition graph was then plotted, and the recovery percentages for each analyte in both buffer and river water was calculated using the corresponding calibration equation.

For the analysis of river water, five vials (50 mL each) of water were collected from the Vltava River (Prague, Czech Republic) at various locations. The samples were mixed and filtered through filter paper (pore size 220 nm). The filtered water was then used to prepare the required buffers and solutions containing desired concentrations of the analytes.

A wastewater sample was collected from Kovohutě (Příbram, Czech Republic), a firm that primarily specializes in recycling lead from lead-acid car batteries. The collected sample was taken prior to any treatment and contains various metal ions and anions. The company's analytical laboratory is accredited for the analysis of these ions using Inductively Coupled Plasma Optical Emission Spectrometry (ICP-OES). The results of the ICP-OES analysis are given in Table S1. Additionally, the sample contains several organic compounds, however, the company is not accredited for their analysis.

Since the sample did not contain $Hg^{2+}$, catechol, or $H_2O_2$, the recovery percentages for these analytes were determined using the standard addition method. The analysis involved spiking the wastewater sample with a known concentration of each analyte, followed by two successive measurements after the addition of further known concentrations. A standard addition graph

was then constructed, and the recovery percentages for each analyte in both buffer and river water were calculated using the corresponding calibration equations.

The analysis of $Pb^{2+}$ ions in the collected sample was similarly performed using the standard addition method. However, since $Pb^{2+}$ was already present in the sample, the initial analysis was carried out on the unspiked wastewater. The results obtained from the standard addition method were then compared with those from the ICP-OES analysis.

| **Table S1**: the results of ICP-OES analysis of wastewater sample | |
|---|---|
| **Substance** | **Concentration /ppm (obtained by ICP-OES)** |
| As | 0.026 |
| Al | 0.032 |
| Ba | 0.060 |
| Cd | 0.398 |
| Cu | 0.011 |
| Fe | 0.292 |
| Mn | 0.396 |
| Ni | 0.654 |
| Pb | 1.63 |
| Sb | <0.05 |
| Sn | <0.02 |
| Tl | 0.062 |
| Zn | 5.28 |
| Li | 0.40 |
| P | 0.099 |
| Cl | 38 |
| S | 1600 |
| pH | 7.0 |
| Conductivity | 3.29 mS $cm^{-1}$ |

*2.3.11 Characterization with SEM and AFM*

SEM was performed by MIRA 2 SEM (TESCAN Ltd., Brno, Czech Republic) To image the electrode's surface, an in-beam secondary electron (SE) detector was used while an accelerating voltage of 25 kV was applied. The working distance was 9 mm, and for scanning mode, an ultrahigh resolution was selected. The measurement was performed in a high vacuum. The elemental analysis was performed on an X-MAX 50 EDX detector (Oxford Instruments plc, Abingdon, UK) under the same conditions, but an external SE detector was used.

A Dimension FastScan atomic force microscopy (AFM) system (JPK NanoWizard Nanooptics ,) with amplitude modulation was employed to assess and study the morphology and surface topography of gold substrates with various modifications. For this means a SCANASYST-AIR cantilever (Bruker AFM Probes, Camarillo, CA, USA) with a BRUKER TESPA-HAR tips was utilized. Subsequently, the raw data gathered from AFM measurements underwent processing and exportation using Gwddyion (a free software).

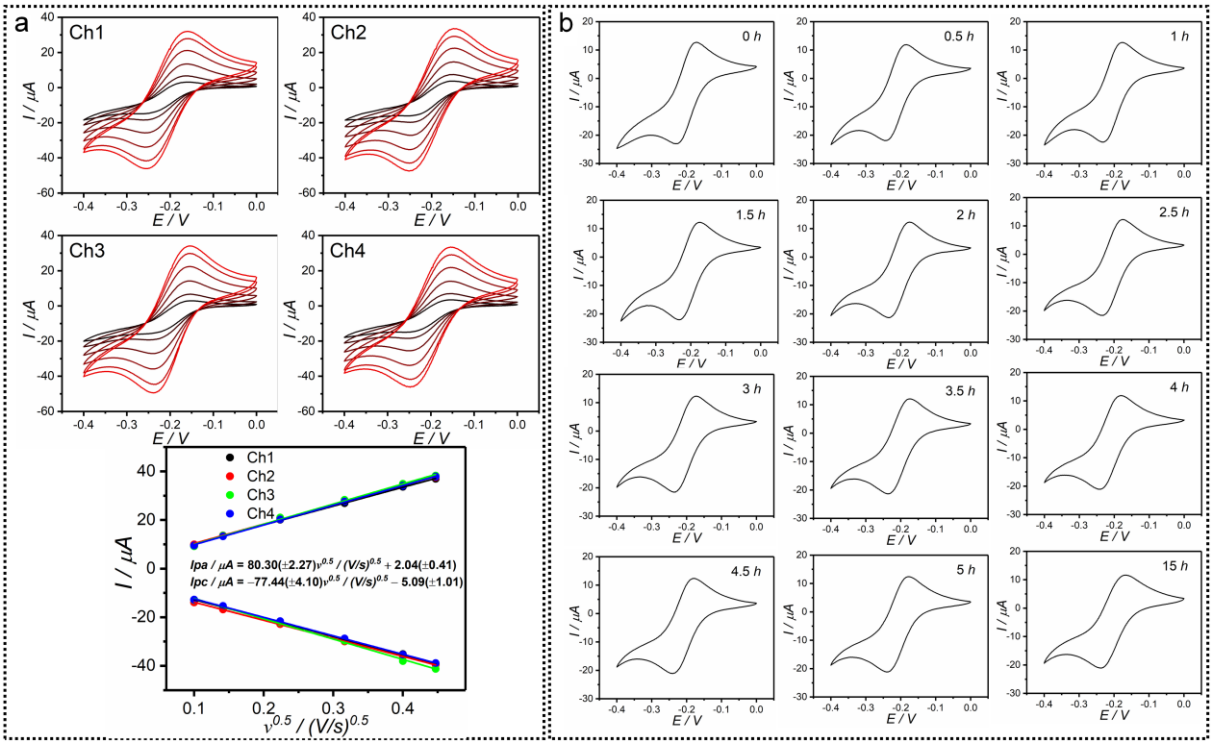


**Figure S1**: *a) The CVs recorded at four channels of fabricated MMEC in 1 mM [Ru (NH)$_3$]$^{2+/3+}$in 100 mM KCl, at various scan rates, 10, 20, 50, 100, 160, and 200 mVs$^{-1}$along with the plot of the dependence of anodic and cathodic peak currents on the square root of scan rate. b) the CVs recorded every half hour in an extended period in 1 mM [Ru (NH)$_3$]$^{3+}$ and 100 mM KCl, scan rate 50 mVs$^{-1}$. After recording each CV the MMEC was rinsed with DI water and left for the desired period and again 1 mM [Ru (NH)$_3$]$^{3+}$ in 100 mM KCl was introduced into the MMEC and the CV was recorded again.*

**Table S2:** The reproducibility between channels evaluated by the RSD% of the anodic and cathodic peak currents across four channels and various scan rates.

| Scan rate | RSD% (*Ipa*) | RSD% (*Ipc*) |
|---|---|---|
| **10 mV $s^{-1}$** | 3.4 | 4.1 |
| **20 mV $s^{-1}$** | 1.3 | 4.3 |
| **50 mV $s^{-1}$** | 2.2 | 2.4 |
| **100 mV $s^{-1}$** | 2.0 | 1.8 |
| **160 mV $s^{-1}$** | 1.5 | 3.6 |
| **200 mV $s^{-1}$** | 1.5 | 2.7 |

**Table S3**: the anodic and cathodic peaks' current values (*Ipa* and *Ipc*) along with peak potential differences ($\Delta E$) of CVs recorded in an extended period.

| ***Time / h*** | ***Ipa / µA*** | ***Ipc / µA*** | ***ΔE / mV*** |
|---|---|---|---|
| 0.0 | 20.4 | 11.3 | 60 |
| 0.5 | 20.3 | 11.1 | 62 |
| 1.0 | 20.4 | 12.6 | 54 |
| 1.5 | 19.6 | 12.9 | 60 |
| 2.0 | 19.0 | 12.8 | 60 |
| 2.5 | 18.7 | 12.9 | 62 |
| 3.0 | 18.5 | 12.9 | 66 |
| 3.5 | 18.3 | 12.9 | 58 |
| 4.0 | 18.2 | 12.6 | 62 |
| 4.5 | 18.2 | 12.8 | 62 |
| 5.0 | 18.2 | 12.8 | 62 |
| 16 | 17.3 | 12.0 | 70 |
| RSD% | 5.4 | 5.2 | 6.37 |

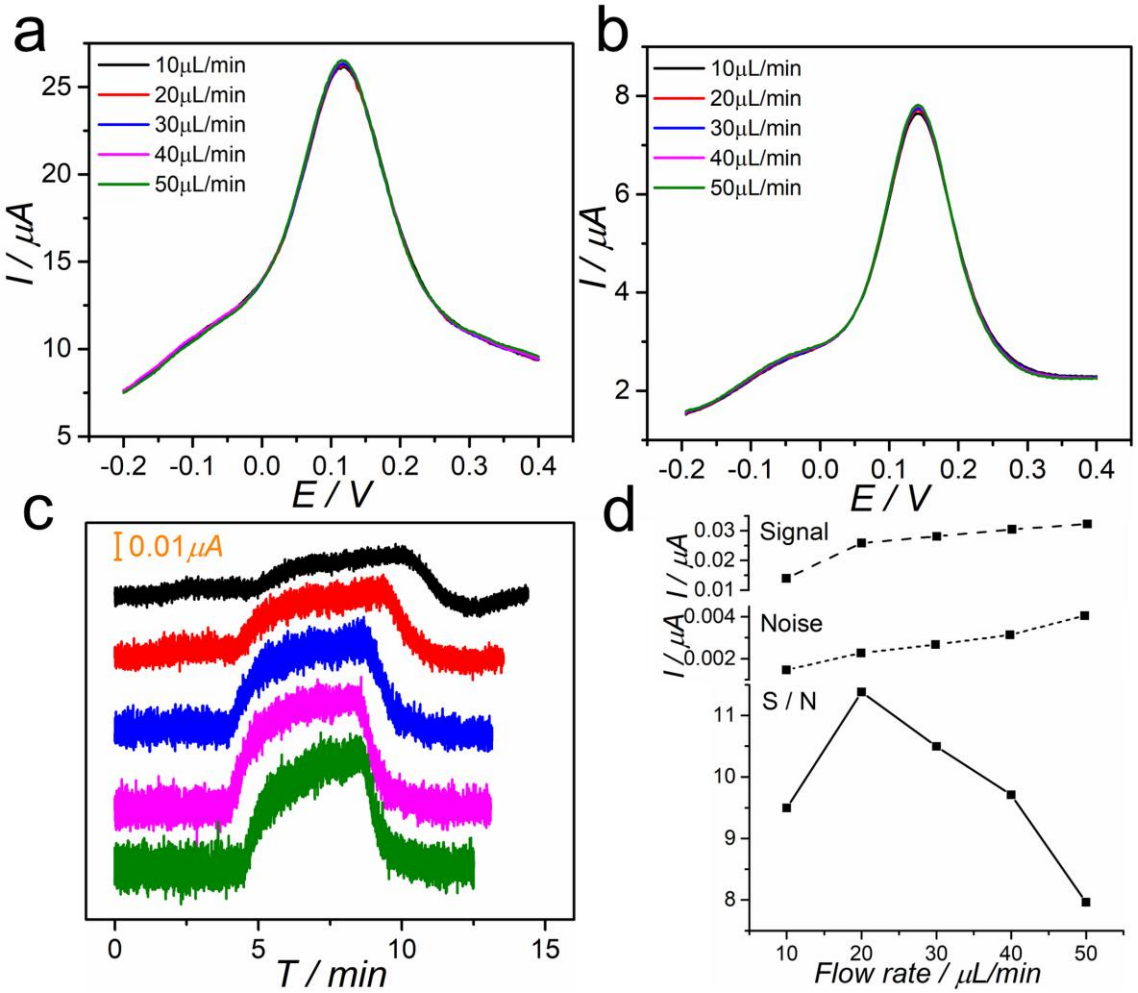


**Figure S2**: *a) the performed DPVs in 0.1 mM of $[Fe(CN)_6]^{4-}$ at different flow rates from 10 to 50 μL $min^{-1}$. b) the performed SWVs in 0.1 mM of $[Fe(CN)_6]^{4-}$ at different flow rates from 10 to 50 μL $min^{-1}$. c) the chronoamperograms recorded at +0.3 V at different flow rates from 10 to 50 μL $min^{-1}$. d) the noise in chronopotentiograms recorded at different flow rates calculated as the standard deviation of the current response before injection of 0.01 mM of $[Fe(CN)_6]^{4-}$. The signal at various flow rates observed upon injection of $[Fe(CN)_6]^{4-}$. The S/N ratio calculated at different flow rates.*

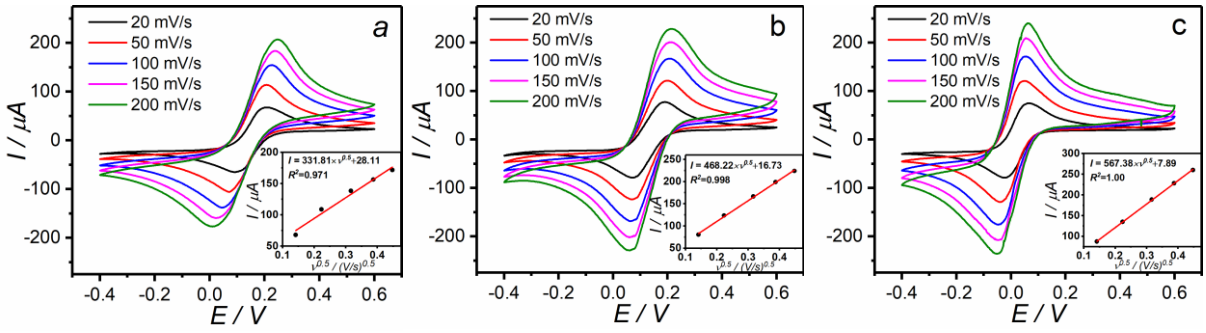


**Figure S3:** *CVs at different scan rates at a) Au, b) Au/AuNS, 10 min electrodeposition of AuNS, and c) Au/PU/AuNS with 2 min electrodeposition of AuNS, electrodes in 4 mM [Fe (CN)$_6$]$^{3-/4-}$ and related scan rate dependence of peak current.*

**Table S4**: The surface properties of electrode configurations obtained by AFM.

| ***Electrode configuration*** | ***scanned area*** | ***RMS roughness (nm)*** | ***Surface area (μm$^2$)*** |
|---|---|---|---|
| ***Bare Au*** | 5 μm×5 μm | 1.1 | 25.1 |
| ***Au/AuNS*** | 5 μm×5 μm | 25.9 | 31.5 |
| ***Au/MF*** | 10 μm×10 μm | 68.5 | 108 |
| ***Au/PU/AuNS*** | 5 μm×5 μm | 15.2 | 34.5 |

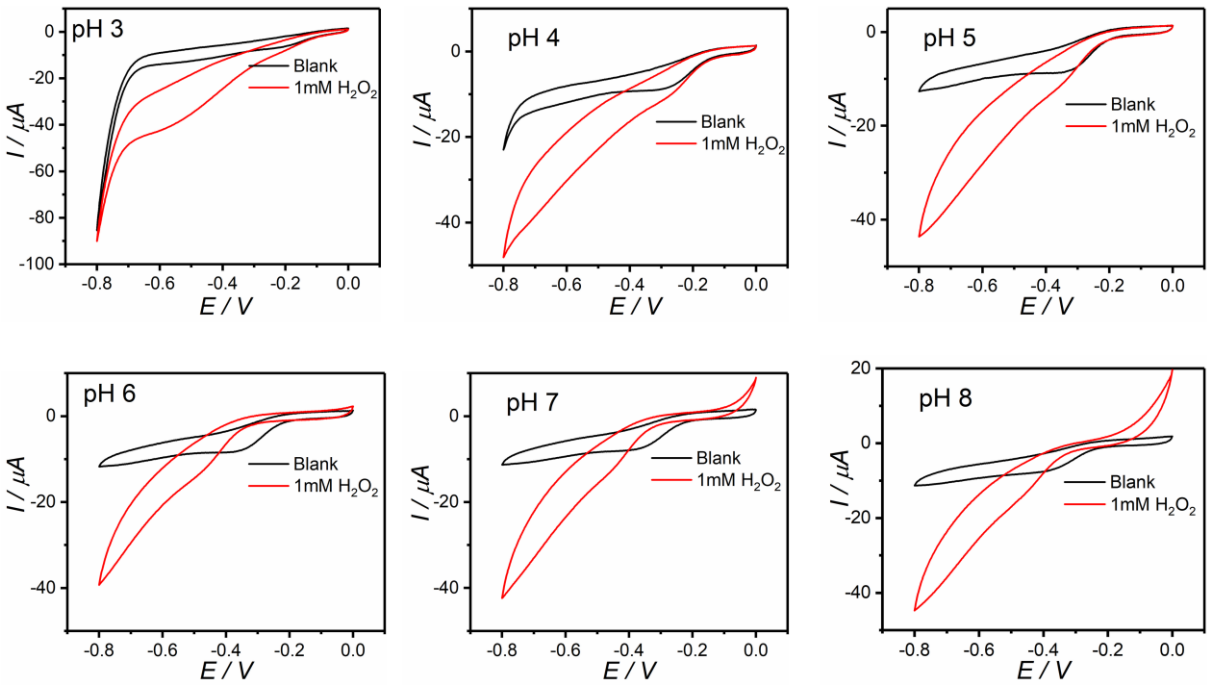


Figure **S4**. *CVs of 1 mM of $H_2O_2$ in Briton Robinson buffer in a pH range from 3 to 8 at Au/AuNS. The scan rate 50 mV $s^{-1}$.*

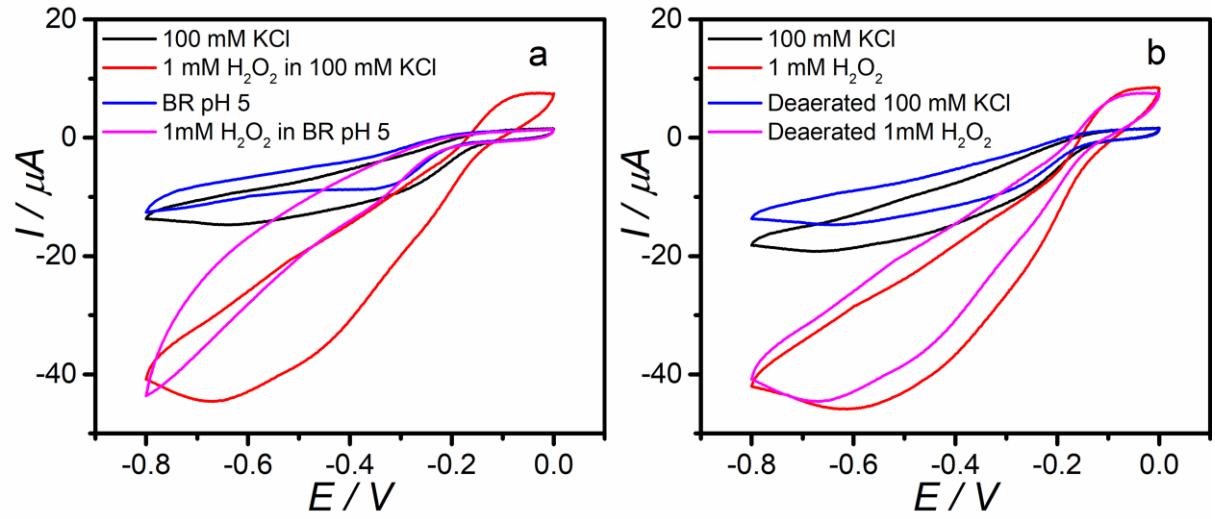


**Figure S5**. *a) CVs of 1 mM of $H_2O_2$ in BR buffer pH 5 and in 0.1 KCl pH 5.2. b) CVs of 1 mM of $H_2O_2$ in deaerated and non-deaerated 0.1 mM KCl.*

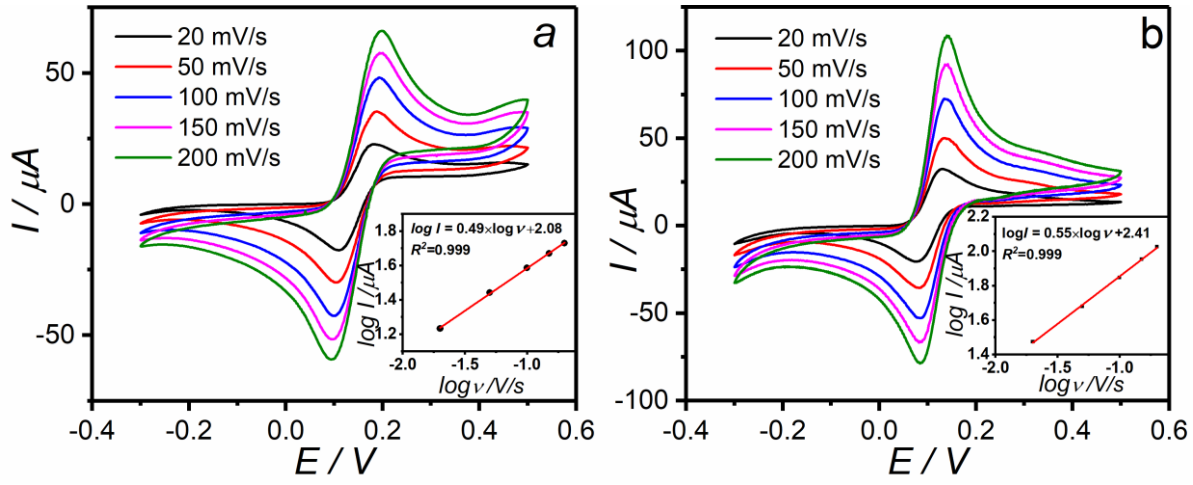


**Figure S6:** *a) CVs of 1 mM of catechol in acetate buffer pH 5.7, at different scan rates (20, 50, 100, 150, and 200 mV/s) at Au electrode, inset shows the logarithm scan rate dependence of anodic peak current. b) CVs of 1 mM of catechol in acetate buffer pH 5.7at different scan rates (20, 50, 100, 150, and 200 mV/s) at Au/PU/AuNS inset shows the scan rate dependence of anodic peak current.*

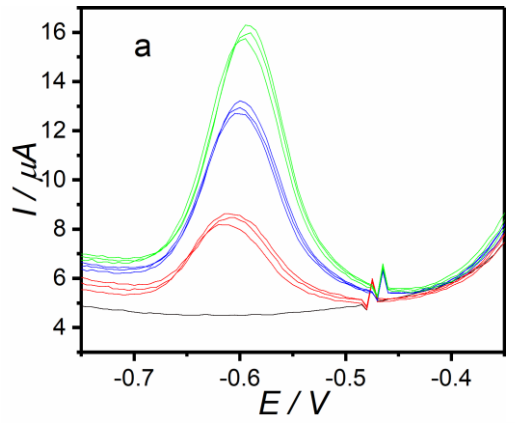
a
I / μA
E / V

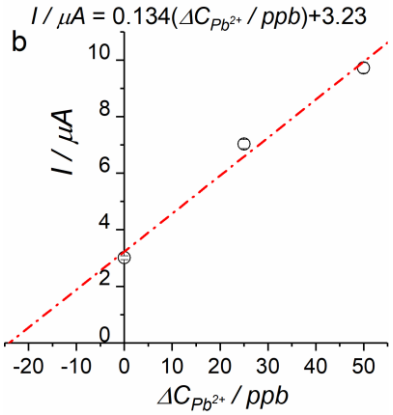
I / μA = 0.134(ΔC_Pb2+ / ppb)+3.23
b
I / μA
ΔC_Pb2+ / ppb

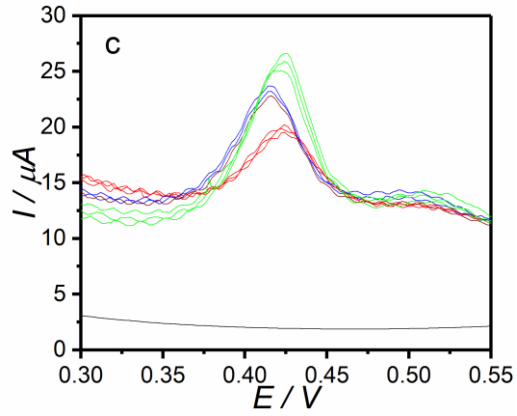
c
I / μA
E / V

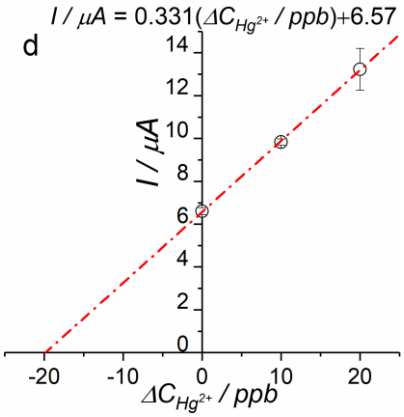
I / μA = 0.331(ΔC_Hg2+ / ppb)+6.57
d
I / μA
ΔC_Hg2+ / ppb

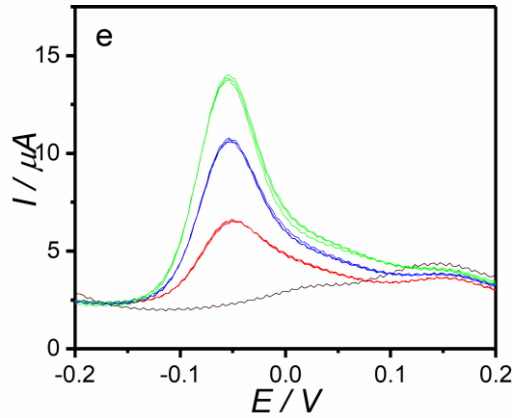
e
I / μA
E / V

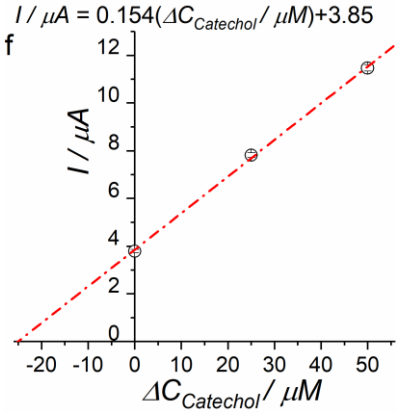
I / μA = 0.154(ΔC_Catechol / μM)+3.85
f
I / μA
ΔC_Catechol / μM

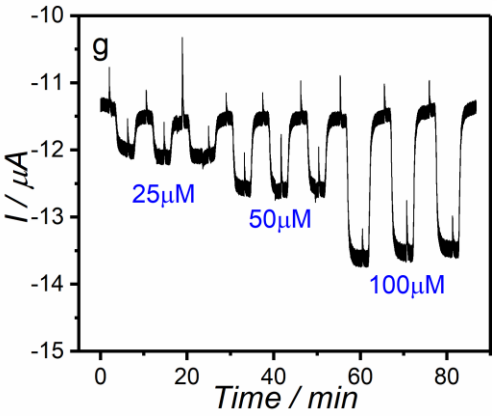
g
25μM
50μM
100μM
I / μA
Time / min

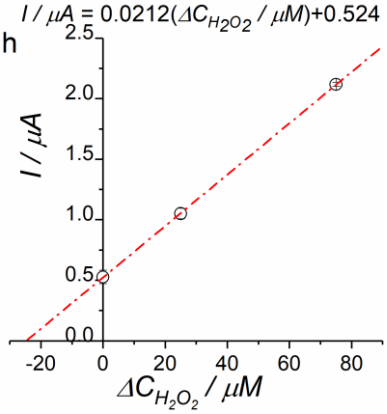
I / μA = 0.0212(ΔC_H2O2 / μM)+0.524
h
I / μA
ΔC_H2O2 / μM

**Figure S7:** *a) ASSWVs of acetate buffer pH 4.5 spiked with 25 ppb of $Pb^{2+}$ followed by two successive additions of 25 and 50 ppb of $Pb^{2+}$ions and b) related standard addition curve. c) ASDPVs of 100 mM of HCl spiked with 20 ppb of $Hg^{2+}$ followed by two successive additions of 10 and 20 ppb of $Hg^{2+}$ions and d) corresponding standard addition curve. e) DPVs of acetate buffer pH 5.7 spiked with 25 µM of catechol and two successive additions of 25 and 50 µM of catechol and f) related standard addition curve. g) chronoamperogram of 100 mM KCl spiked with 25 µM of $H_2O_2$ followed by two successive additions of 25 and 75 µM of $H_2O_2$ and h) related standard addition curve.*

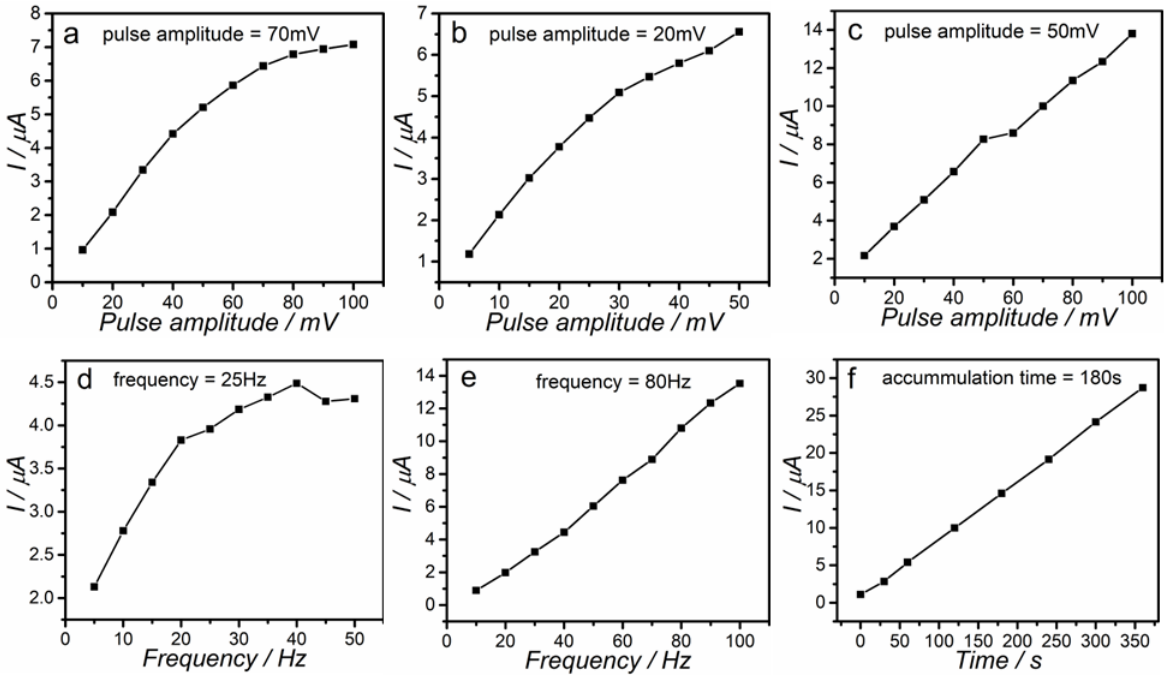


**Figure S8**: *the optimization of parameters for each analyte. The pulse amplitude for a) $Hg^{2+}$ ions determination, b) catechol determination, c) $Pb^{2+}$ ions determination. Frequency of applied pulse for d) catechol, and e) $Pb^{2+}$ ions. f) accumulation time for $Hg^{2+}$ determination.*

**Table S5:** Selected electrochemical systems designed for multiplexed analysis

| Analyte | Electrochemical technique | Electrode | Number of chamber/channel | Reusability | Counter/ reference electrode | Potentiostat | Microfluidic system | Parallel/Time division measurement | Ref. |
|---|---|---|---|---|---|---|---|---|---|
| Lactate, Paracetamol, Lithium, | DPV, Amperometry potentiometry | Multiple SPEs | 4 | Disposable | Separate | Multichannel potentiostat (4) | No | Parallel | [45] |
| Glucose, Lactate | Amperometry | Thread-based electrode | 2 | Disposable | Separate | Multichannel potentiostat (16) | No | Parallel | [46] |
| Prostate specific antigen , Interleukin 8 | CV, Amperometry | SPE array | 16 | Disposable | Separate | Multichannel potentiostat (16) | No | Parallel | [47] |
| pH and Oxygen | Potentiometry, Chronoamperometry | Thread-based electrode | 2 | Reuseable | Shared | Multichannel potentiostat (2) | Yes | Time-division | [48] |
| L-tyrosine | DPV | Multiple SPEs | 10 | Limited reusability | Separate | Single channel-Potentiostat (1) | No | Time-division | [49] |
| Escherichia coli, Pseudomonas aeruginosa, Proteus mirabilis, Staphylococcus aureus | Amperometry | Gold electrodes sputtered on plastic | 16 | Disposable | Separate | Multichannel potentiostat (2) | No | Time-division | [50] |
| Glucose, Lactate, Oxygen | Amperometry | screen-printed multianalyte sensor | 8 | | Shared | Multichannel potentiostat (2) | Yes | Parallel | [51] |

*Corresponding authors: ashrafi@ufe.cz, homola@ufe.cz

| | | | | | | | | | |
|---|---|---|---|---|---|---|---|---|---|
| Nitric oxide, Peroxynitrite | Amperometry | Gold ultramicroelectrodes patterned on glass by thermal evaporation | | Disposable | Shared | Multichannel potentiostat (2) | No | Parallel | [52] |
| Carcinoembryonic antigen, α-fetoprotein, β-human choriogonadotropin, Carcinoma antigen 125 | Amperometry | SPEs | 4 | Disposable | Shared | Multichannel potentiostat (4) | No | Parallel | [53] |
| Carcinoembryonic antigen, α-fetoprotein, Cancer antigen 125, Carbohydrate antigen 153 | DPV | Screen-printed paper-electrodes. | 8 | Disposable | Shred | Single channel potentiostat (1) | Yes | Time-division | [54] |
| $Pb^{2+}$ and $Hg^{2+}$ ions, catechol, $H_2O_2$ | ASSWV, ASDPV, DPV, Chronoamperometry | Gold electrodes on glass by vacuum evaporation | 4 | High reusability | Separate | 4 independent potentiostats | Yes | Parallel | This work |

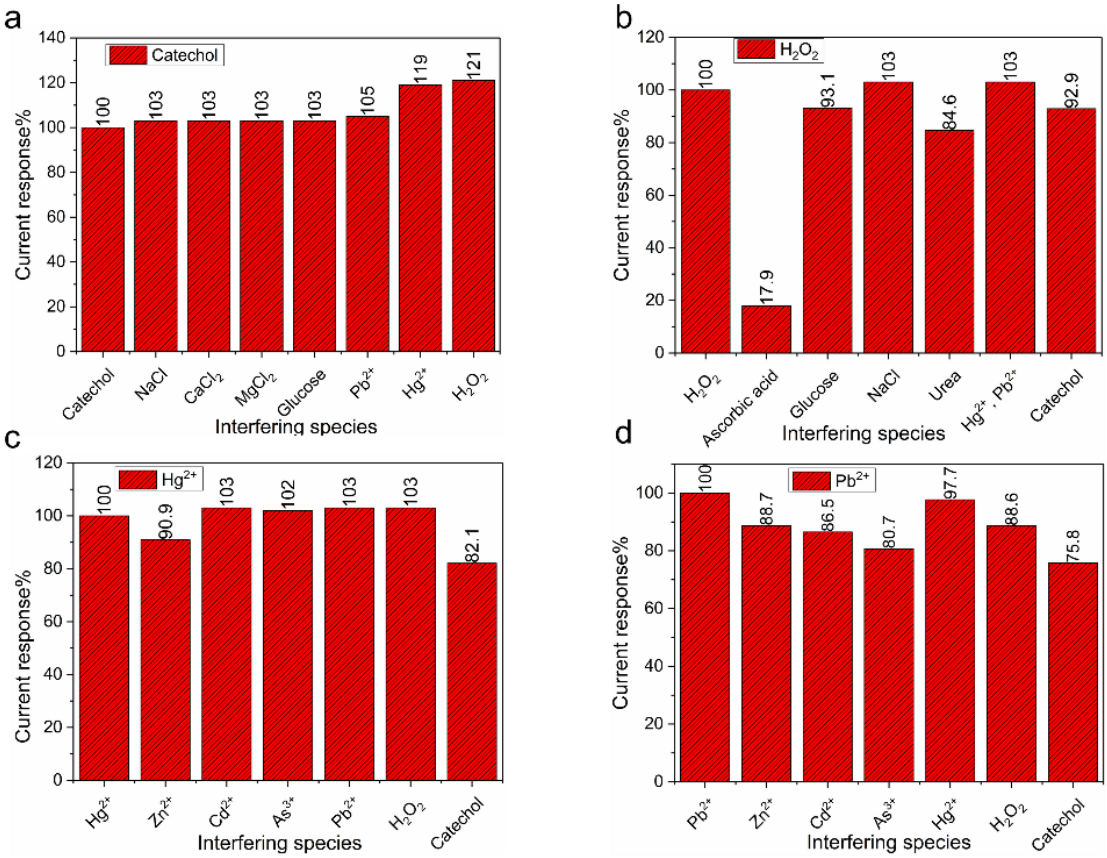


**Figure S9**: *The effect of potential interfering species on the current response of different analytes. a) 50 µM of catechol and with addition of 50 µM NaCl, 50 µM $CaCl_2$, 50 µM $MgCl_2$, 50 µM glucose, 50 ppb $Pb^{2+}$, 50 ppb $Hg^{2+}$, and 50 µM $H_2O_2$. b) 50 µM $H_2O_2$ and with addition of 50 µM of ascorbic acid, 50 µM glucose, 50 µM NaCl, 50 µM urea. 50 ppb of $Pb^{2+}$, 50ppb $Hg^{2+}$, and 50 µM of catechol. c) 50 ppb $Hg^{2+}$ and with addition of 50 ppb $Zn^{2+}$, 50 ppb $Cd^{2+}$, 50 ppb $As^{3+}$, 50 ppb $Pb^{2+}$, 50 µM $H_2O_2$, and 50 µM of catechol. d) 50 ppb $Pb^{2+}$ and with addition of 50 ppb $Zn^{2+}$, 50 ppb $Cd^{2+}$, 50 ppb $As^{3+}$, 50 ppb $Hg^{2+}$, 50 µM $H_2O_2$, and 50 µM of catechol.*

*Corresponding authors: ashrafi@ufe.cz, homola@ufe.cz

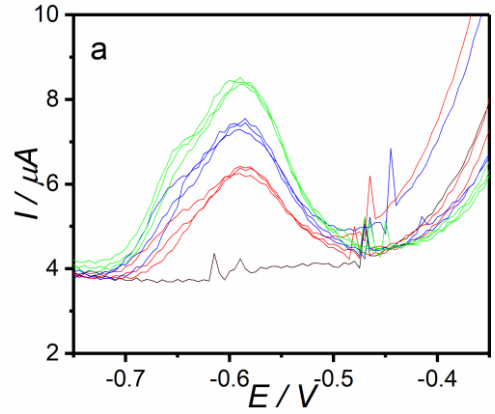
a
I / μA
E / V

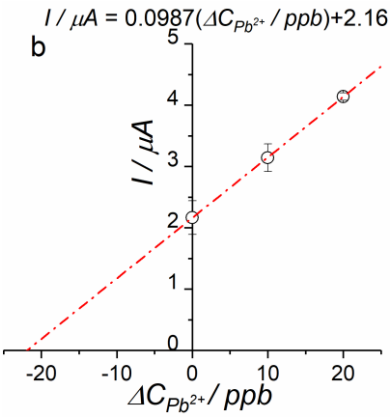
I / μA = 0.0987(ΔC_Pb2+ / ppb)+2.16
b
I / μA
ΔC_Pb2+ / ppb

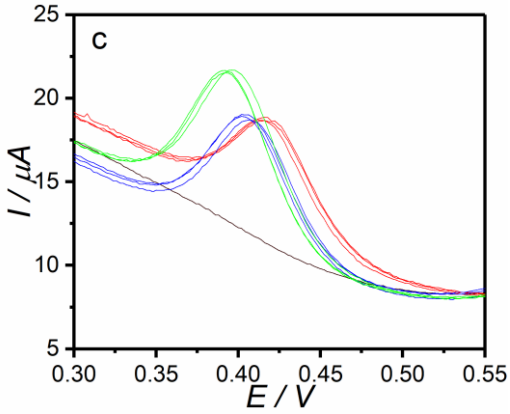
c
I / μA
E / V

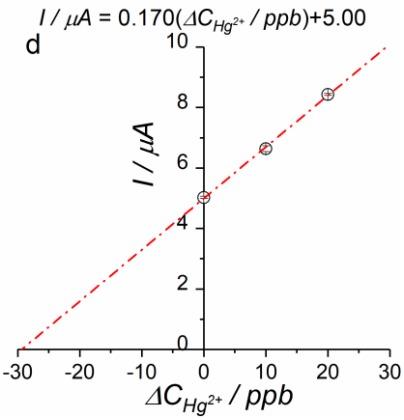
I / μA = 0.170(ΔC_Hg2+ / ppb)+5.00
d
I / μA
ΔC_Hg2+ / ppb

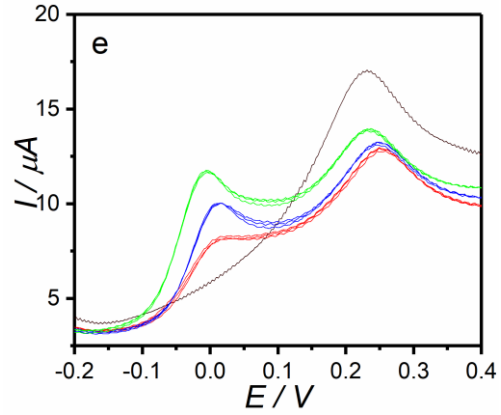
e
I / μA
E / V

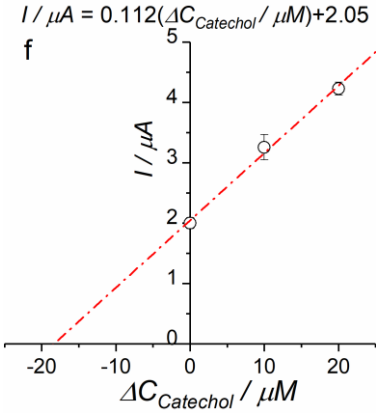
I / μA = 0.112(ΔC_Catechol / μM)+2.05
f
I / μA
ΔC_Catechol / μM

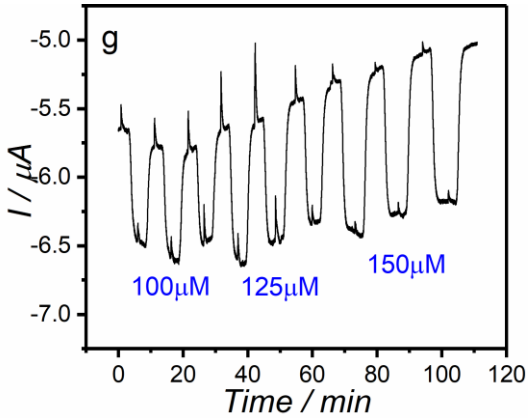
g
I / μA
100μM
125μM
150μM
Time / min

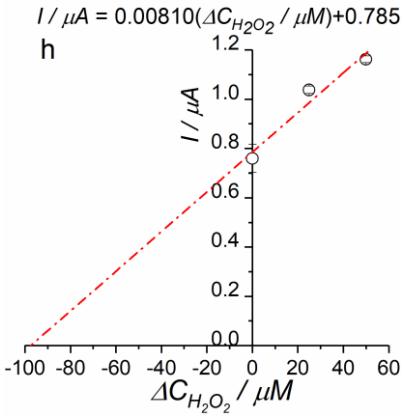
I / μA = 0.00810(ΔC_H2O2 / μM)+0.785
h
I / μA
ΔC_H2O2 / μM

**Figure S10:** *a) ASSWVs of river water sample diluted (2×) in acetate buffer pH 4.5 and spiked with 20 ppb of $Pb^{2+}$ followed by two successive additions of 10 and 20 ppb of $Pb^{2+}$ ions, and b) related standard addition curve. c) ASDPVs of river water sample diluted (2×) in 100 mM of HCl and spiked with 30 ppb of $Hg^{2+}$ followed by two successive additions of 10 and 20 ppb of $Hg^{2+}$ ions and d) related standard addition curve. e) DPVs of river water sample diluted (2×) in acetate buffer pH 5.7 and spiked with 20 µM of catechol and two successive additions of 10 and 20 µM of catechol and f) related standard addition curve. g) chronoamperogram of river water sample diluted (2×) in 100 mM KCl and spiked with 100 µM of $H_2O_2$ followed by two successive additions of 25 and 50 µM of $H_2O_2$ and h) related standard addition curve.*

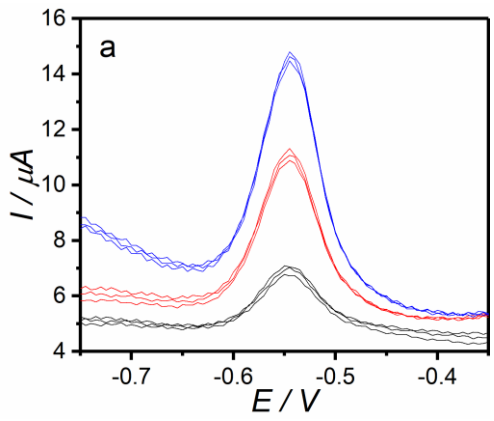
a
I / μA
E / V

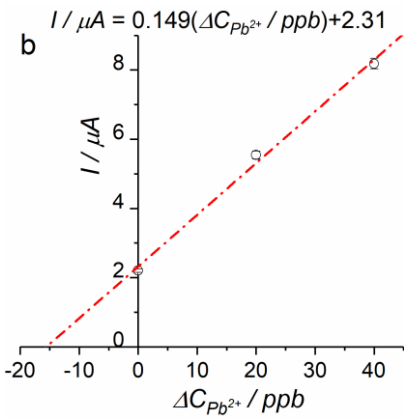
I / μA = 0.149(ΔC_Pb2+ / ppb)+2.31
b
I / μA
ΔC_Pb2+ / ppb

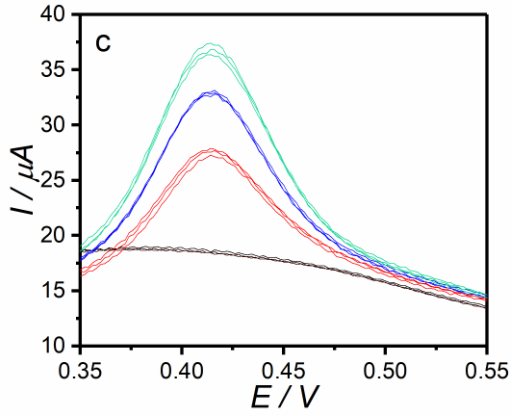
c
I / μA
E / V

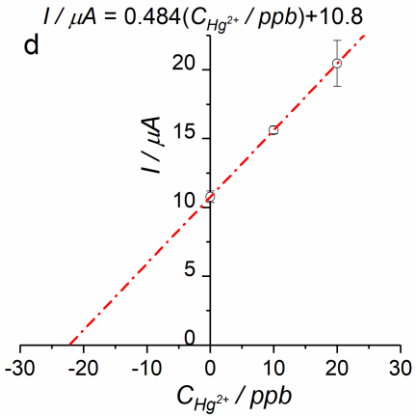
I / μA = 0.484(C_Hg2+ / ppb)+10.8
d
I / μA
C_Hg2+ / ppb

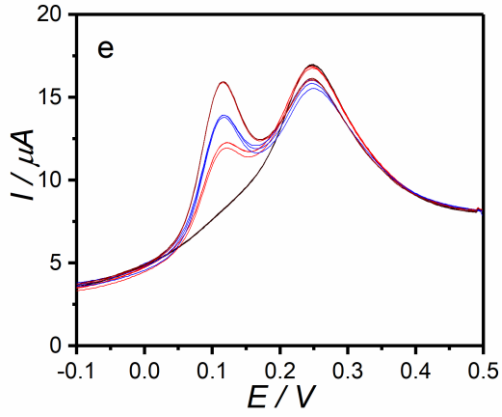
e
I / μA
E / V

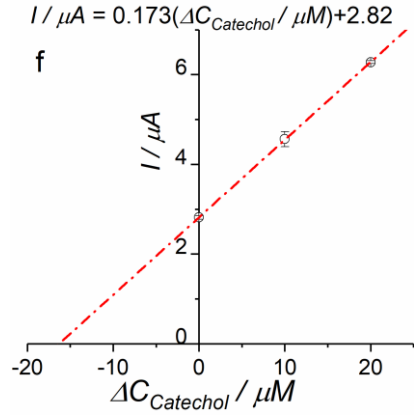
I / μA = 0.173(ΔC_Catechol / μM)+2.82
f
I / μA
ΔC_Catechol / μM

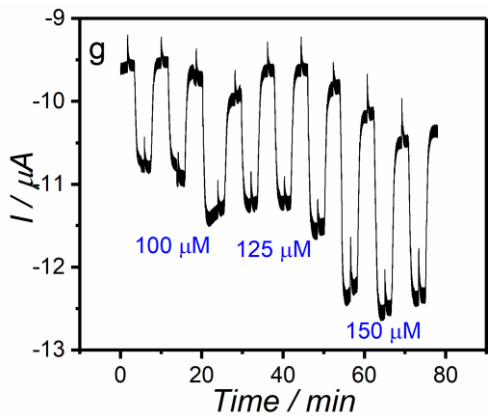
g
I / μA
100 μM
125 μM
150 μM
Time / min

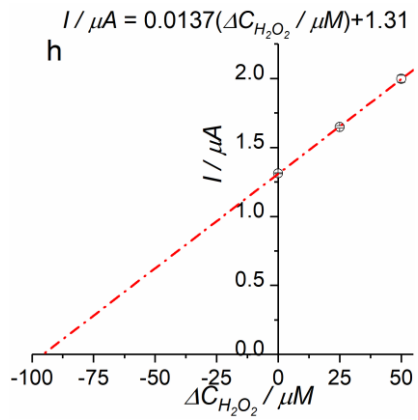
I / μA = 0.0137(ΔC_H2O2 / μM)+1.31
h
I / μA
ΔC_H2O2 / μM

**Figure S11:** *a) ASSWVs of wastewater sample diluted (100×) in acetate buffer pH 4.5 followed by two successive additions of 20 and 40 ppb of* $Pb^{2+}$ *ions, and b) related standard addition curve. c) ASDPVs of wastewater sample diluted (50×) in 100 mM of HCl and spiked with 20 ppb of* $Hg^{2+}$ *followed by two successive additions of 10 and 20 ppb of* $Hg^{2+}$ *ions and d) related standard addition curve. e) DPVs of wastewater sample diluted (50×) in acetate buffer pH 5.7 and spiked with 20 µM of catechol and two successive additions of 10 and 20 µM of catechol and f) related standard addition curve. g) chronoamperogram of wastewater sample diluted (50×) in 100 mM KCl and spiked with 100 µM of* $H_2O_2$ *followed by two successive additions of 25 and 50 µM of* $H_2O_2$ *and h) related standard addition curve.*